FEMS Yeast Research, 21, 2021, foaa070

doi: 10.1093/femsyr/foaa070
Advance Access Publication Date: 23 December 2020
Research Article

RESEARCH ARTICLE

Physical, genetic and functional interactions between the eisosome protein Pil1 and the MBOAT O-acyltransferase Gup1

Joana Tulha[1], Mariana Amorim-Rodrigues[1,2], Lidia Alejo Esquembre[3], Sebastien Rauch[4], Markus J. Tamás[3] and Cândida Lucas[1,2,*,†]

[1]Centre of Molecular and Environmental Biology, University of Minho, Campus de Gualtar 4710-057 Braga, Portugal, [2]Institute of Science and Innovation for Bio-Sustainability (IB-S), University of Minho, Campus de Gualtar 4710-057 Braga, Portugal, [3]Department of Chemistry and Molecular Biology, University of Gothenburg, Kemihuset 412 96 Gothenburg, Sweden and [4]Water Environment Technology, Department of Architecture and Civil and Environmental Engineering, Chalmers University of Technology, S-412 96 Gothenburg, Sweden

*Corresponding author: Institute of Science and Innovation for Bio-Sustainability (IB-S), University of Minho, Campus of Gualtar, 4710-057 Braga, Portugal. Tel: +351-253-601-584/80; E-mail: clucas@bio.uminho.pt

One sentence summary: Yeast MBOAT *O*-acyltransferase Gup1 interacts physically, genetically and functionally with the eisosomal Pil1, and has a role in eisosome formation and cell wall integrity, and during arsenite and acetate stress.

Editor: Cristina Mazzoni

†Cândida Lucas, http://orcid.org/0000-0001-8605-4525

ABSTRACT

The *Saccharomyces cerevisiae* MBOAT *O*-acyltransferase Gup1 is involved in many processes, including cell wall and membrane composition and integrity, and acetic acid-induced cell death. Gup1 was previously shown to interact physically with the mitochondrial membrane VDAC (Voltage-Dependent Anion Channel) protein Por1 and the ammonium transceptor Mep2. By co-immunoprecipitation, the eisosome core component Pil1 was identified as a novel physical interaction partner of Gup1. The expression of *PIL1* and Pil1 protein levels were found to be unaffected by *GUP1* deletion. In Δ*gup1* cells, Pil1 was distributed in dots (likely representing eisosomes) in the membrane, identically to *wt* cells. However, Δ*gup1* cells presented 50% less Pil1-GFP dots/eisosomes, suggesting that Gup1 is important for eisosome formation. The two proteins also interact genetically in the maintenance of cell wall integrity, and during arsenite and acetic acid exposure. We show that Δ*gup1* Δ*pil1* cells take up more arsenite than wt and are extremely sensitive to arsenite and to acetic acid treatments. The latter causes a severe apoptotic *wt*-like cell death phenotype, epistatically reverting the Δ*gup1* necrotic type of death. Gup1 and Pil1 are thus physically, genetically and functionally connected.

Keywords: *Saccharomyces cerevisiae*; co-immunoprecipitation; Gup1 Pil1; eisosomes; cell wall; arsenite

INTRODUCTION

The yeast Gup1 protein, which belongs to the MBOAT family of *O*-acyltransferases, affects many cellular processes in a yet unknown biochemical fashion (Lucas *et al.* 2016). The *Saccharomyces cerevisiae GUP1* deleted strains are best described in association with cell wall composition and stability (Ferreira *et al.* 2006, 2010), with lipid metabolism and functionality (Oelkers *et al.* 2000), with implications in glycosylphosphatidylinositol (GPI)-anchor remodeling (Bosson, Jaquenoud and Conzelmann 2006) and with membrane structure, particularly with

Received: 29 September 2020; **Accepted:** 21 December 2020

the assembly and integrity of lipid ordered domains/rafts (Ferreira and Lucas 2008). Other evidence supports the involvement of Gup1 in cytoskeleton polarization, intracellular trafficking and vacuole morphology (Lucas *et al.* 2016). *GUP* genes have been found in virtually all eukaryotic genomes sequenced so far. In higher eukaryotes, Gup1 (designated as HHATL) was described to operate as a negative regulator of the Hedgehog pathway (Abe, Kita and Niikura 2008), important in developmental processes regulating morphogenesis, differentiation and patterning, and in proliferation and cell fate during embryogenesis and wound healing (Varjosalo and Taipale 2007; Lee, Zhao and Ingham 2016). Morphogenesis phenotypes have been associated with *GUP1* deletion in the fungal pathogen *Candida albicans*, which upon deletion of the two *GUP1* copies loses virulence and the corresponding ability to differentiate, adhere, invade and form biofilms (Ferreira *et al.* 2010). Moreover, the deletion of *GUP1* in *S. cerevisiae* impairs acetic acid-induced regulated cell death (RCD) (Tulha *et al.* 2012). Thus, a better understanding of the Gup1, its interaction partners and cellular functions might be useful for future development of antifungal drugs.

Yeast Gup1 localizes to the plasma membrane, to the Endoplasmic reticulum (ER) (Holst *et al.* 2000; Bleve *et al.* 2005) and to the mitochondria (Holst *et al.* 2000; Tulha and Lucas 2018). These multiple localizations suggest multiple functions and multiple partners. Accordingly, Gup1 has been shown to physically interact with the yeast mitochondrial membrane VDAC protein Por1 (Tulha and Lucas 2018) and the plasma membrane-localized ammonium transceptor Mep2 (Van Zeebroeck *et al.* 2011). Whole-genome screenings (SGD database) suggest a larger physical interactome that, nevertheless, requires confirmation. The Gup1–Por1 partnership is involved in the processes of RCD in response to acetic acid, and cell wall integrity maintenance in response to injury-causing drugs (Tulha and Lucas 2018). On the other hand, the Gup1–Mep2 partnership affects *MEP2* expression, as well as proper membrane distribution and transport activity of Mep2 (van Zeebroeck *et al.* 2011). In view of the extensive phenotypes associated with *GUP1* deletion and the multiple intracellular localizations of Gup1 (Lucas *et al.* 2016), the present work aimed at identifying novel physical interaction partners using the co-immunoprecipitation (Co-IP) methodology previously proven successful (Tulha and Lucas 2018). Under non-stress physiological conditions, the protein Pil1, an eisosome core structural protein (Walther *et al.* 2006; Olivera-Couto *et al.* 2011), was identified as a physical partner of Gup1. The present work shows that the *GUP1* deleted mutant has ∼50% less eisosomes than *wt* cells.

Eisosomes act as sensors of changes in membrane tension, with consequences in the response to stress caused by environment, nutrition, and plasma membrane and cell wall perturbing conditions and agents (reviewed by Lanze *et al.* 2020). These responses include changes in (i) cell wall composition and integrity, (ii) lipid homeostasis, (iii) plasma membrane architecture and related cell signaling, (iv) morphogenesis, (v) resistance to antifungal drugs and (vi) the manifestation of several virulence factors. All of these were previously described in association with *GUP1* deletion in *S. cerevisiae* and/or *C. albicans* (reviewed by Lucas *et al.* 2016). The results in this current study show that Gup1 and Pil1 interact genetically and functionally in cell wall integrity. The interaction of these proteins also has consequences in the sensitivity to arsenite, and in acetic acid-promoted RCD.

MATERIALS AND METHODS

Strains and growth conditions

The yeast strains used in this study are listed in Table 1. Yeasts were cultivated on YPD (1% yeast extract (Panreac AppliChem, Spain), 2% peptone (BD Difco, France), 2% glucose (LabChem, Portugal), or YNB without amino acids and nitrogen (BD Difco, France) (0.175%), with 0.5% $(NH_4)_2SO_4$ (Panreac AppliChem, Spain) and 2% glucose, supplemented according to auxotrophic requirements. Batch liquid cultures were grown at 30°C and 200 rpm orbital shaking in a 1:3 liquid-to-air ratio. Solid media contained 2% agar.

Constructions

The plasmids used in this work derived from pYES2 vector (Invitrogen/Thermo Scientific, USA) and were previously described: pYES-*GFP* (Tulha and Lucas 2018) and pYES2-*GUP1-GFP* (Bleve *et al.* 2011). The double mutant *S. cerevisiae* Δ*gup1* Δ*pil1* was constructed by replacing the *GUP1* gene in BY4741 Δ*pil1* (*MAT***a** *ura3*Δ*0 leu2*Δ*0 his3*Δ*1 met15*Δ*0* YGR086c::kanMX4 from Euroscarf, Germany) with the *HIS3* disruption cassette amplified from the p416 GPD plasmid (ATCC® 87360) using the primers A and B in Table S1 (Supporting Information), by homologous recombination using standard protocols (Ito *et al.* 1983). Transformants were selected in YNB with 2% glucose and supplements without histidine (Panreac AppliChem, Spain). Positive clones were confirmed by colony PCR (polymerase chain reaction) using the primers C and D in Table S1 (Supporting Information). Strain BY4741 Δ*gup1 PIL1*-GFP was constructed by deleting the *GUP1* gene from the BY4741 Δ*pil1 PIL1-GFP* strain (Huh *et al.* 2003), using the KanMx disruption cassette amplified from plasmid pUG6 (Euroscarf), using the primers E and F in Table S1 (Supporting Information), by homologous recombination as above. Transformants were selected in YNB with 2% glucose and supplements with geneticin (Gibco, Thermo Fisher Scientific) (200 mg/L). Positive clones were confirmed by colony PCR using the primers C and G listed in Table S1 (Supporting Information).

Co-immunoprecipitation methodology

The Co-IP procedure and the protein identification were performed as described before (Tulha and Lucas 2018). Peptide mass fingerprinting and MALDI-TOF was purchased from the Unidad de Proteómica, Parque Científico de Madrid, UCM.

Microscopy

Fluorescence microscopy was done in a Leica Microsystems DM-5000B epifluorescence microscope with the GFP Filter (Ex Bp 470/40 and Em Bp 525/40), and a 100× oil-immersion objective. Images were acquired through a Leica DCF350FX digital camera and processed with LAS AF Leica Microsystems image software. The same system was used to observe and photograph cells by light microscopy. All the data in this work derive from observing at least 300 living cells per independent batch and at least three batches. Cells were cultivated and collected as mentioned in the text/legends.

qRT-PCR

Total RNA isolation and qRT-PCR procedures were done as described in Tulha and Lucas (2018) using the primers listed in

Table 1. Yeast strains used in this study. (ns: non specified)

Strain	Genotype	Source
S. cerevisiae W303-1A *wt*	MATa *leu2-3112 trp1-1 can1-100 ura3-1 ade2-1 his3-11,15*	ns
S. cerevisiae W303-1A Δ*gup1*	MATa *leu2-3112 trp1-1 can1-100 ura3-1 ade2-1 YGL084c::HIS5*	Holst *et al.* (2000)
S. cerevisiae W303-1A Δ*gup1* pYES2 Ø	MATa *leu2-3112 trp1-1 can1-100 ura3-1 ade2-1 YGL084c::HIS5* [pYES2(*URA3*)]	Tulha and Lucas (2018)
S. cerevisiae W303-1A Δ*gup1* pYES2-*GFP*	MATa *leu2-3112 trp1-1 can1-100 ura3-1 ade2-1 YGL084c::HIS5* [pYES2(*URA3*)]	Tulha and Lucas (2018)
S. cerevisiae W303-1A Δ*gup1* pYES2-*GUP1-GFP*	MATa *leu2-3112 trp1-1 can1-100 ura3-1 ade2-1 YGL084c::HIS5* [pYES2(*URA3*)]	Tulha and Lucas (2018)
S. cerevisiae BY4741 *wt*	MATa *ura3Δ0 leu2Δ0 his3Δ1 met15Δ0*	Euroscarf
S. cerevisiae BY4741 Δ*gup1*	MATa *ura3Δ0 leu2Δ0 his3Δ1 met15Δ0 YGL084c::kanMX4*	Euroscarf
S. cerevisiae BY4741 Δ*pil1*	MATa *ura3Δ0 leu2Δ0 his3Δ1 met15Δ0 YGR086C::kanMX4*	Euroscarf
S. cerevisiae BY4741 Δ*gup1*Δ*pil1*	MATa *ura3Δ0 leu2Δ0 met15Δ0 YGR086C::kanMX4 YGL084c::HIS3*	This study
S. cerevisiae BY4741 Δ*pil1PIL1-GFP*	MATa *ura3Δ0 leu2Δ0 met15Δ0 YGR086C::PIL1-GFP-HIS3*	Huh *et al.* (2003)
S. cerevisiae BY4741 Δ*gup1*Δ*pil1PIL1-GFP*	MATa *ura3Δ0 leu2Δ0 his3Δ1 met15Δ0 YGR086C::PIL1-GFP-HIS3 YGL084c::kanMX4*	This study

Table S2 (Supporting Information). The mRNAs quantification was normalized to the *18S* gene. The comparative Ct method analysis ($2^{-\Delta\Delta CT}$ method) (Schmittgen and Livak 2008) was used to analyze the results.

Western blotting

Yeasts were cultivated in 5 mL YPD at 30°C and 200 rpm orbital shaking up to OD_{600nm} 1.0, and were collected by centrifugation (5 min at 5000 rpm). The pellet was resuspended in 200 μL of 0.2 M NaOH (Sigma-Aldrich, Germany) with 2% β-mercaptoethanol (Promega) and precipitated with 400 μL 20% trichloroacetic acid (Panreac AppliChem, Spain), washed with 500 μL acetone and solubilized in 100 μL 2× loading buffer [5× loading buffer (10% w/v SDS, 10 mM β-mercaptoethanol, 20% v/v glycerol (Sharlau, Spain), 0.2 M Tris–HCl (Sigma-Aldrich, Germany) pH 6.8, 0.05% w/v bromophenol blue (Sigma-Aldrich, Germany)) diluted with 1× Tris-EDTA (TE) buffer]. Samples were run on a 10% SDS–PAGE, transferred to a PVDF membrane (Roche, Portugal) (54 mA 1.5 h), blocked with 5% non-fat milk in phosphate-buffered saline (PBS) containing 0.05% Tween 20 (Sigma-Aldrich, Germany), and incubated overnight at 4°C with the primary antibody mouse monoclonal anti-GFP 1:2 500 (Roche, Portugal) and mouse monoclonal anti-Pgk1 (cytoplasmic phosphoglycerate kinase) 1:10 000 (Invitrogen/Thermo Scientific, USA). Dilutions of the antibodies were prepared using the above blocking mix. Membranes were incubated at room temperature for 1.5 h with secondary antibody against mouse IgGs (1:10 000) (Sigma-Aldrich, Germany), revealed by chemiluminescence (Amersham ECL, GE Healthcare, USA) according to the manufacturer's instructions, and visualized in a ChemiDoc equipment (XMS BioRad).

Phenotypic assessment

Drop tests

Drop tests were performed using cell suspensions at $OD_{600} = 1$, collected from mid-exponential YPD grown cultures ($OD_{600} = 0.6$–0.8). Four 10-fold serial dilutions in sterile water were made, and 5 μL of each suspension was applied on solid YPD, YPG (YP with 2% w/v glycerol), YPE (YP with 2% v/v ethanol (Carlo Erba, France)) or YPD supplemented as described in the text. Results were scored after 3 days of incubation at 30°C, unless otherwise stated.

Sensitivity to high amounts of acetic acid

Yeast strains were grown until mid-exponential growth phase ($OD_{600} = 0.6$–0.8) on YNB with 2% glucose and supplements and resuspended to a final $OD_{600} = 0.2$ in identical fresh medium, adjusted to pH 3.0 with HCl and containing 150 mM of acetic acid (Panreac AppliChem, Spain). Incubation took place for 180 min at 30°C. At determined time points, 40 μL from a 10^{-4} cell suspension were inoculated onto YPD agar plates and colony forming units (c.f.u.) were counted after 48 h incubation at 30°C. The percentage of viable cells was estimated considering 100% survival as the number of c.f.u. obtained at time 0 (T_0). The integrity of the membrane of cells exposed to acetic acid was assessed as previously described (Tulha *et al.* 2012), i.e. after incubation with acetic acid, cells were harvested, washed and resuspended in PBS containing 4 μg/mL propidium iodide (PI) (Sigma-Aldrich, Germany), incubated for 10 min at room temperature in the dark and analyzed in an Epics ® XL (Beckman Coulter) flow cytometer. A minimum of 20 000 cells from each sample were analyzed per experiment.

Sensitivity to arsenite

Cells growing exponentially in YNB with 2% glucose and supplements at an $OD_{600} = 1$, were serially diluted 10-fold, and 5 μL of each suspension was applied onto plates supplemented with 2% glucose in the absence or presence of sodium arsenite [As(III)] at the indicated concentrations. Growth was monitored after 2–3 days at 30°C.

Arsenic uptake

Exponentially growing cells in YNB with 2% glucose and supplements were either untreated or exposed to 1 mM As(III) for 1 h, collected and washed twice in ice-cold water. The cell pellet was resuspended in water, boiled for 10 min and centrifuged to collect the supernatant. The arsenic content of each sample was determined by ICP-MS. Prior to analysis, the samples were diluted 20 times using water from a GenPure water purification system (Thermo Scientific, Barnstead, resistivity 18.2 MΩ cm) and acidified to 1% volume HNO_3 (Sharlau, nitric acid 65% for trace analysis). The analysis was performed on an iCAP Q ICP-MS (Thermo Fisher Scientific, USA) with an SC-FAST automated sampling introduction system (Elemental Scientific, USA). The instrument was operated in the Kinetic Energy Discrimination (KED) mode with He as the collision gas to remove potential interference from argon chloride. Calibration was performed using a set of As standards with concentrations up to 500 $\mu g\,L^{-1}$.

A 1 $\mu g L^{-1}$ indium solution was continuously injected for internal standardization. The detection limit estimated based on six blank analyses was 0.1 μg As L^{-1}.

RESULTS AND DISCUSSION

Pil1 is a physical partner of Gup1; implications in the number of eisosomes

Previously, two Gup1 physical partners were identified, the plasma membrane ammonium transceptor Mep2 (van Zeebroeck *et al.* 2011) and the mitochondrial VDAC Por1 (Tulha and Lucas 2018). Por1 was found by co-immunoprecipitating Gup1-GFP with an anti-GFP antibody, while Mep2 was found using a split-ubiquitin two-hybrid system. Using this last approach, specifically adapted for membrane proteins, Miller *et al.* (2005) presented a HTP assay in which ±30% of the *S. cerevisiae* annotated membrane proteins including Gup1, did not display any interaction with other proteins or themselves. Bearing in mind these discrepancies, the former Co-IP approach (Tulha and Lucas 2018) was chosen to search for further putative Gup1 partners. This was done using solubilized protein lysates of *S. cerevisiae* W303 cells expressing this Gup1-GFP chimeric protein under the control of the strong galactose-induced GAL1 promoter (Bleve *et al.* 2005; Tulha and Lucas 2018). Its induction for 16 h caused extensive membrane/ER proliferation (Bleve, di Sansebastiano and Grieco 2011). This was obviated by using a galactose-induction time of 6 h, which neither displayed membrane proliferation structures (Tulha and Lucas 2018), nor caused the release of fluorescence into the vacuole (not shown). Silver stained sodium dodecyl sulphate–polyacrylamide gel electrophoresis (SDS-PAGE) of the results from one such assay (Fig. 1), shows several new protein bands. These were excised and analyzed by Peptide Mass Fingerprinting using MALDI-TOF. Only one band yielded an unequivocal answer: a protein of ~38 kDa that was identified as Pil1 (score 63, covering 39% of the amino acid sequence) (Fig. 1).

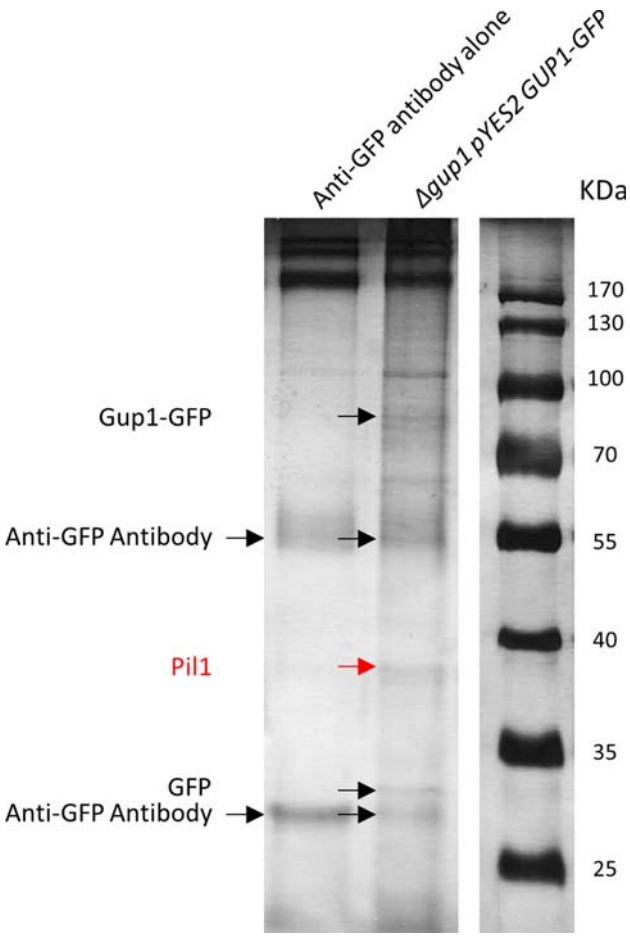

Figure 1. SDS-PAGE of the Co-IP assay. Co-IP of whole cell lysates of *S. cerevisiae* W303–1A Δ*gup1* expressing Gup1-GFP using an anti-GFP antibody (lane 2). Control SDS-PAGE of the antibody alone suspended in loading buffer (lane 1). Bands were excised and identified by LC-MS/MS.

Pil stands for phosphorylation inhibited by long-chain bases. Pil1 is a member of the BAR domain protein family (Habermann 2004), which comprises proteins that contribute to shape membrane curvatures, participating in the early steps of endocytosis and sensing. Pil1 and Lsp1, another BAR domain protein, form the eisosome structural core (Walther *et al.* 2006; Olivera-Couto *et al.* 2011). Eisosomes configure furrow-like invaginations of the plasma membrane that aggregate thousands of Pil1 and Lsp1 molecules (Ziółkowska *et al.* 2011; Douglas and Konopka 2014; Olivera-Couto *et al.* 2015). These proteins directly bind to lipids and form a curved structure that locates in the cytoplasmic side of MCC domains (membrane compartment containing Can1) (Malínská *et al.* 2004; Strádalová *et al.* 2009; Malínský, Opekarová and Tanner 2010; Douglas *et al.* 2011; Douglas and Konopka 2014; Foderaro, Douglas and Konopka 2017). Pil1 interacts electrostatically with the negatively charged phosphoinositide phosphatidylinositol (4,5)-biphosphate (PI(4,5)P2), concentrated in the cytoplasmic layer of MCC domains (Olivera-Couto *et al.* 2011; Ziółkowska *et al.* 2011), forcing the membrane to bend (Foderaro, Douglas and Konopka 2017). MCCs are also rich in complex lipids and ergosterol (Douglas *et al.* 2011; Foderaro, Douglas and Konopka 2017).

Gup1 is a membrane protein with 11–12 transmembrane domains (Holst *et al.* 2000). Many of the previously described phenotypes associated with the deletion of *GUP1* are associated with the plasma membrane (Lucas *et al.* 2016). Besides the changes in lipid composition (Oelkers *et al.* 2000), the Δ*gup1* mutant displays (i) an even distribution of ergosterol (Ferreira and Lucas 2008), (ii) the mislocalization of the Pma1 proton pump and (iii) inefficient Stl1-mediated glycerol/H^+ symport (Ferreira *et al.* 2005). All of these, including the malfunction of active permeases, were previously associated with eisosome disassembly through *PIL1* deletion (Malínská *et al.* 2003; 2004; Grossmann *et al.* 2007; 2008). Eisosomes harbor numerous sensors, signaling effectors and transporters, and play important roles in regulation and signaling-associated processes, as well as in membrane organization (Douglas *et al.* 2011; Foderaro, Douglas and Konopka 2017; Moharir *et al.* 2018). The Pil1 sub-cellular distribution/localization was therefore assessed in the Δ*gup1* mutant comparing to *wt* cells, using the strains expressing the chromosomal chimeric insertion Pil1-GFP, as a mean to assess the integrity, distribution and number of eisosomes.

In the *wt* strain, Pil1-GFP distributed as expected in punctate patches (Fig. 2A), likely corresponding to the eisosomes (Moreira *et al.* 2009; Strádalová *et al.* 2009). This type of distribution was preserved in the Δ*gup1* mutant (Fig. 2A). However, in the absence of Gup1, the number of these Pil1 associated-punctate structures, which are widely used to quantify the number of eisosomes per cell (e.g. Moreira *et al.* 2009; Strádalová *et al.* 2009), was found to be significantly reduced (Fig. 1B). More than 300 cells from each of ≥3 independent batches of Δ*gup1* and *wt* were

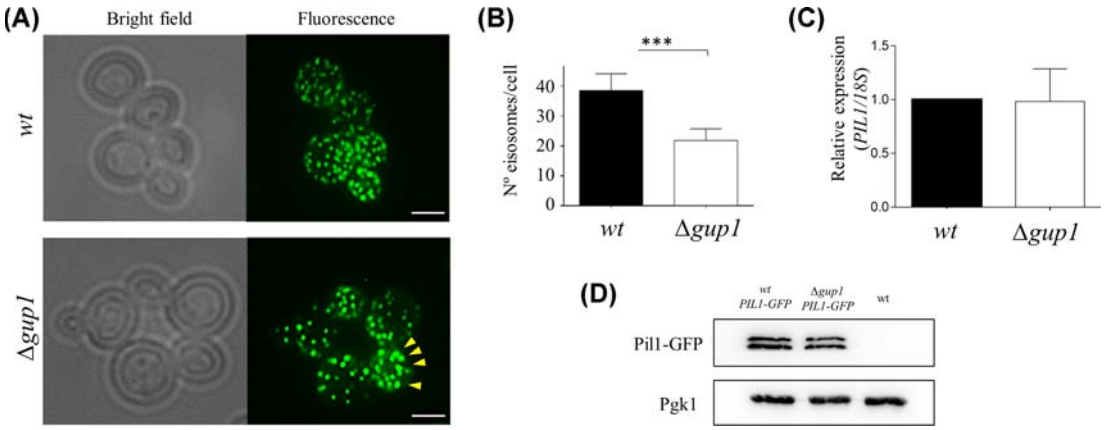

Figure 2. Effects of deleting *GUP1* from S. *cerevisiae* BY4741 on the subcellular localization and distribution of Pil1 **(A)**, the number of eisosomes/cell **(B)** and the expression of *PIL1* **(C)**. Cells were cultivated in YNB with 2% glucose and supplements until mid-exponential growth phase. (A) Pil1-GFP chromosomal insertion shows the location and distribution of Pil1 in live cells. Arrows indicate fluorescent dots bigger than average. Bars = 5 μm. (B) The number of eisosome structures was counted in 300 cells per experiment. Results are representative of at least three independent experiments. $^{***}P < 0.001$ *t*-test. (C) Relative expression of *PIL1* by qRT-PCR. *PIL1* expression was normalized against *18S* and represented relative to the levels in the *wt* strain as calculated by the comparative Ct method analysis (2-ΔΔCT method). **(D)** Western blotting of anti-GFP antibody against whole protein extracts from Δ*pil1PIL1*-GFP (positive control), Δ*gup1* Δ*pil1 PIL1*-GFP and *wt* (negative control). Loading control was made using anti-Pgk1 antibody.

quantified in this fashion. The *wt* and the Δ*gup1* mutant presented 38.6 ± 5.7 and 21.9 ± 3.9 eisosomes/cell, respectively, i.e. the mutant had ∼56% less eisosomes than the *wt* strain. Noticeably, some of the Pil1-GFP punctate patches in Δ*gup1* cells appeared bigger than average (arrows in Fig. 2A). The cause of such a significantly reduced number of eisosomes was further investigated. A small number of eisosomes has been associated with reduced amounts of Pil1 protein (Moreira *et al.* 2009). Therefore, the expression of *PIL1* in the Δ*gup1* strain was quantified by qRT-PCR and found to be identical to that in *wt* cells (Fig. 2C). Additionally, the relative amounts of Pil1-GFP protein in Δ*gup1* mutant and *wt* cells were assessed by western blotting using an anti-GFP antibody confirming that the amounts of protein are similar in both strains (Fig. 2D). These results suggest that *PIL1* expression is not affected by the absence of Gup1, and that the reduced number of eisosomes per cell observed in the Δ*gup1* strain is not a direct consequence of a reduction in Pil1 protein levels.

The deletion of *GUP1* causes profound alteration in membrane lipid composition (Oelkers *et al.* 2000; Bosson, Jaquenoud and Conzelmann 2006) and organization/structure (Bosson, Jaquenoud and Conzelmann 2006; Ferreira and Lucas 2008). The mutant has less phospholipids, and more diacyl- and triacylglycerols (Oelkers *et al.* 2000) and lyso-PI (Bosson, Jaquenoud and Conzelmann 2006). Thus, it is possible that the absence of Gup1 influences the number of eisosomes by decreasing the available amounts of PI(4,5)P2. Eisosomes have been proposed to maintain phosphoinositide homeostasis, particularly that of PI(4,5)P2 (Fröhlich *et al.* 2014; Kabeche *et al.* 2014, Kabeche, Howard and Moseley 2015b). The other way round, membrane association of Pil1 with PI(4,5)P2 was proposed to be the limiting step in eisosome formation (Moreira *et al.* 2009; Olivera-Couto *et al.* 2011). Accordingly, the reduction of PI(4,5)P2 causes a decrease in the total number of eisosomes (Karotki *et al.* 2011; Kabeche *et al.* 2015a). This is therefore a possibility to be explored in the future.

Genetic interactions between Gup1 and Pil1

To evaluate the extent of the effect of the interaction between Gup1 and Pil1, the double mutant Δ*gup1* Δ*pil1* was created. Single and double mutants and *wt* were used to assay some of the most prominent phenotypes previously associated with Δ*gup1* (Lucas *et al.* 2016). These phenotypes were assessed in the same culture conditions as before, many of which rely on cultivating the cells on glucose. Previous work using the Δ*end3–1* mutant suggested that Gup1 is internalized by endocytosis when the cells are shifted to glucose (Bleve *et al.* 2005). Yet, the expression of *GUP1* remains almost constant under glucose repression or derepression conditions (Oliveira and Lucas 2004; Lewis *et al.* 2014; Kunkel, Luo and Capaldi 2019), suggesting that if endocytosis occurs, the protein is probably swiftly replaced, supporting the numerous *GUP1* deletion phenotypes observed before.

Effect of cell wall-injuring drugs

Cells were grown in the presence of cell wall-damaging drugs such as Calcofluor White (CFW), caffeine and Congo Red (CR). CFW and CR bind cell wall chitin, thereby interfering with proper cell wall assembly (Roncero and Durán 1985; Ram and Klis 2006). These drugs operate differently, as inferred from distinct transcriptional profiles induced by either drug (Kuranda *et al.* 2006). CR induces the alteration of the expression of a small group of genes, almost completely restricted to cell wall remodeling functions (Kuranda *et al.* 2006), suggesting it specifically affects the Cell Wall Integrity (CWI/PKC) pathway. CFW on the other hand, triggers both HOG and CWI/PKC pathways (Alonso-Monge *et al.* 1999; García-Rodriguez, Durán and Roncero 2000). It alters the expression of a larger set of genes from RNA metabolism, transport, organelle biogenesis and the response to stress (Kuranda *et al.* 2006). Caffeine affects TORC1-mediated activation of the CWI pathway (Lum *et al.* 2004; Kuranda *et al.* 2006).

Results of growth on YPD at 30°C in the presence of these drugs (Fig. 3A, left) show that Δ*gup1* has a strong CFW sensitivity consistent with a primary defect in cell wall biogenesis and composition (Ferreira *et al.* 2006). CR, on the other hand, surprisingly affected more the *wt* than the Δ*gup1* mutant. This was unexpected since CR binds chitin in the cell wall and Δ*gup1* has 90% more chitin than *wt* cells (Ferreira *et al.* 2006). Possibly, the high amount of chitin in the mutant cell wall might cause a saturation-derived limit for the effect of CR. The Δ*pil1* mutant did not show any significant sensitivity to CFW or CR in comparison with the *wt*. However, the Δ*gup1* Δ*pil1* double mutant

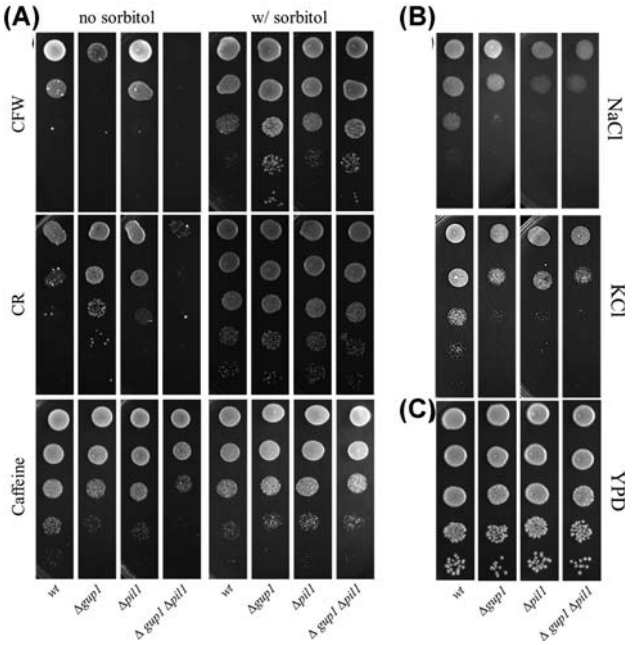

Figure 3. (A) Phenotypes of *S. cerevisiae* BY4741 *wt*, Δ*gup1*, Δ*pil1* and Δ*gup1* Δ*pil1* strains in response to cell wall-injuring chemicals, CR—Congo Red (100 mg/L), CFW—Calcofluor White (50 μg/mL) and caffeine (12 mM). Osmotic remediation of the phenotypes was tested with 1 M sorbitol. Results were scored after 3 days of incubation at 30°C. **(B)** Identical assays in YPD supplemented with 1 M NaCl or 1.5 M KCl. **(C)** Control assay in YPD. One representative experiment is shown.

was unable to grow in the presence of either drug, and was 10-fold more severely affected by caffeine than either single mutant (Fig. 3A, left). The osmotic stabilization of the cells by 1-mM sorbitol (Levin 2005) restored growth (Fig. 3A, right). Taken together, these results indicate that Gup1 and Pil1 affect related processes at the level of the cell wall.

A role (direct or indirect) of eisosomes in the regulation of the synthesis of cell wall components, as well as their spatial distribution, has been suggested (Foderaro, Douglas and Konopka 2017), possibly independently of the CWI/PKC pathway (Ferreira *et al.* 2006; Wang *et al.* 2011). The Δ*gup1* mutant appears to be responding regularly at the level of CWI/PKC pathway Slt2 phosphorylation (Ferreira *et al.* 2006) and, consistently (Munro *et al.* 2007; Lenardon *et al.* 2009), it has 90% more chitin than *wt* (Ferreira *et al.* 2006). Although there is no information available on the composition of cell wall in the Δ*pil1* strain, it is known that Pil1 complexes with β-1,3-glucan synthase Fks1 (Gavin *et al.* 2002), allowing to expect that the Δ*pil1* mutant is affected in glucan synthesis as reported to occur in other eisosome mutants (Wang *et al.* 2011; Foderaro, Douglas and Konopka 2017). The extreme effect of CFW and CR, and the exacerbated effect of caffeine on Δ*gup1* Δ*pil1* show that the cell wall is severely affected when the two proteins Gup1 and Pil1 are absent, to the point of impairing growth. This confirms that eisosomes are crucial for the maintenance of the wall integrity as previously suggested (Foderaro, Douglas and Konopka 2017). Particularly, the effect of caffeine suggests that the TORC1-mediated CWI/PKC activation is affected, possibly at the level of steps that are common to CFW and CR responses (Wanke *et al.* 2008).

Effect of hyperosmotic salt stress

There is solid evidence for cooperative cross-talk between HOG and PKC/CWI pathways in cell wall biogenesis (Rodriguez-Peña *et al.* 2010). Namely, HOG controls the basal expression of several cell wall proteins as well as chitin synthetases (Lenardon *et al.* 2009). Transcription of the PKC/CWI effector *SLT2* in response to high osmolarity seems to be dependent on both Hog1 and the PKC/CWI pathway-governed transcription factor Rlm1 (Rodríguez-Peña *et al.* 2010). To assess the ability of the mutants to withstand high osmotic stress, the single and double mutants were grown on YPD and YNB with 2% glucose and supplements with 1 M NaCl or 1.5 M KCl (Fig. 3B). The three mutants showed moderate and equal sensitivity to these salts in comparison to the *wt* strain. The Δ*gup1* mutant is moderately sensitive to salt stress, in association with defective intake of glycerol for osmoregulation purposes (Holst *et al.* 2000; Ferreira *et al.* 2005). Moreover, MCC eisosome domains have been associated with the response to stress injuries, including hyper and hypoosmotic stress (Dupont *et al.* 2010; Berchtold *et al.* 2012; Kabeche, Howard and Moseley 2015b). The observation that both single and double mutants have the same sensitivity to osmotic stress suggests that Gup1 and Pil1 might act in the same pathway during hyperosmotic stress response. A possible pathway might include the aquaglyceroporin Fps1 that closes in response to hyperosmotic stress to promote the retention of glycerol. A failure to close Fps1 renders cells sensitive to high osmolarity (Tamás *et al.* 1999).

Growth in the presence of arsenite and arsenite influx

In addition to its role in glycerol transport across the plasma membrane, Fps1 also mediates uptake of the metalloid arsenic in form of trivalent arsenite [As(III)] into cells (Wysocki *et al.* 2001). To test whether Gup1 and Pil1 might affect Fps1, we grew cells in the presence of sodium arsenite. Deletion of *GUP1* causes a strong sensitivity to As(III), which is aggravated in the Δ*gup1* Δ*pil1* mutant (Fig. 4A), while growth of the Δ*pil1* mutant was largely unaffected. The intracellular amounts of arsenic were measured after 1 h incubation with 1 mM As(III). The double mutant accumulated ∼50% more arsenic than the *wt* and the single mutants (Fig. 4B). Thus, in the absence of both *GUP1* and *PIL1*, cells accumulate more arsenic and become highly sensitive to this metalloid. The aquaglyceroporin Fps1 is the main entry pathway of As(III) in cells growing on glucose (Wysocki *et al.* 2001). Previous studies have shown that Fps1 activity is regulated by the MAP kinases of the HOG (Hog1) and CWI/PKC (Slt2) pathways (Thorsen *et al.* 2006; Ahmadpour *et al.* 2016). Likewise, Hog1 and Slt2 are activated by As(III) (Thorsen *et al.* 2006; Ahmadpour *et al.* 2016; Lee and Levin 2018). The present results suggest that Fps1 might be deregulated (i.e. more of the Fps1 molecules are open) in the double mutant, allowing a higher influx of As(III). Fps1 also mediates the entry of acetic acid into cells (Mollapour and Piper 2007; Lindahl *et al.* 2017). Thus, if Fps1 does not close properly in the Δ*gup1* Δ*pil1* mutant, it should allow the entrance of more acetic acid, promoting increased sensitivity of the double mutant to this compound leading to faster/stronger death of the cells.

Acetic acid-induced cell death

Previously, we showed that the *GUP1* deleted mutant is greatly sensitive to acetic acid, although it dies with features that are more necrosis- than apoptosis-like, in opposition to what is observed for *wt* cells (Tulha *et al.* 2012). The previously reported physical association of Gup1 with the mitochondrial inner membrane VDAC Por1 (Tulha and Lucas 2018), was shown to be implicated in that process. Therefore, the strains used in this study were challenged with acetic acid apoptosis-inducing conditions.

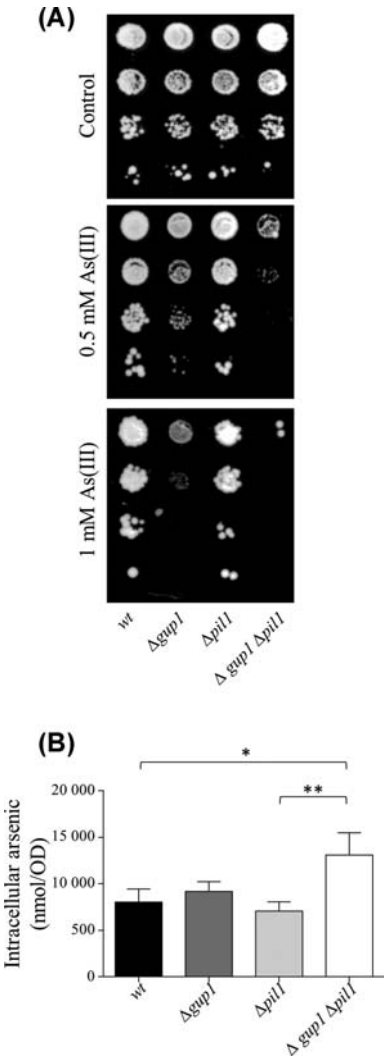

Figure 4. (A) Phenotypes of *S. cerevisiae* BY4741 *wt*, Δ*gup1*, Δ*pil1* and Δ*gup1* Δ*pil1* strains in the presence of sodium arsenite [As(III)]. Results were scored in YNB with 2% glucose and supplements after 3 days of incubation at 30°C. **(B)** Intracellular arsenic. Cells were exposed to 1 mM As(III) during 1 h, washed and intracellular arsenic content measured in three independent biological replicas. Data represent mean ± standard deviation of at least three independent experiments. $^{**}P < 0.01$; $^{*}P < 0.1$ one-way ANOVA followed by Tukey Mean Difference test.

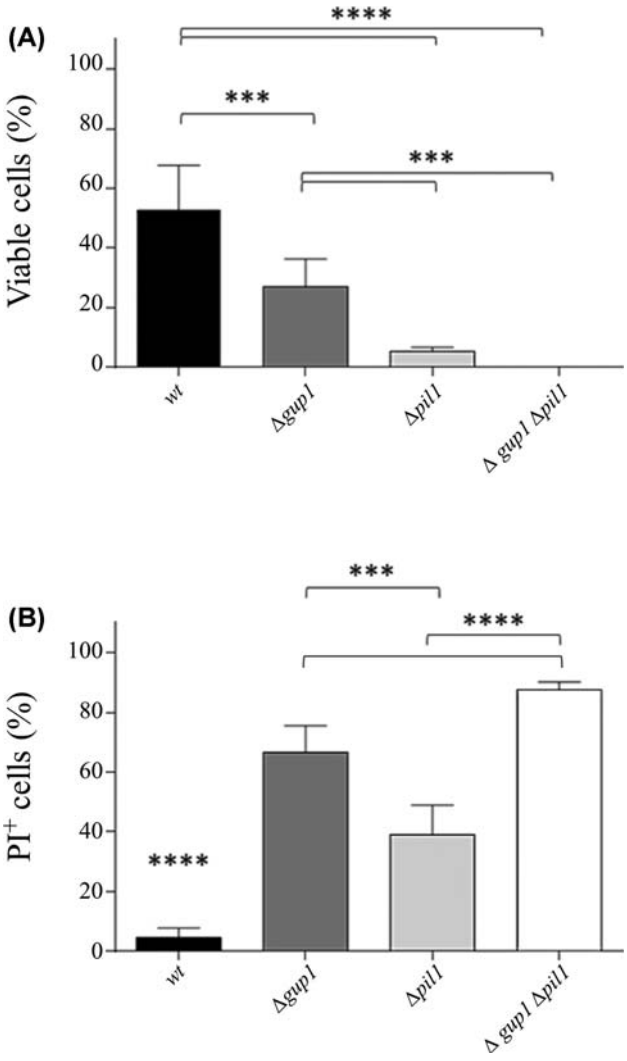

Figure 5. Response of *S. cerevisiae* BY4741 *wt*, Δ*gup1*, Δ*pil1* and Δ*gup1* Δ*pil1* strains to acetic acid-induced cell death. Exponentially growing cells on YNB with 2% glucose and supplements were treated with 150 mM acetic acid for 3 h. **(A)** Viability was determined by c.f.u. assay (results were normalized with 100% survival corresponding to the total c.f.u. at T_0). **(B)** Graphic representation of the percentage of cells displaying positive PI staining, assessed by flow cytometry. Data represent mean ± standard deviation of at least three independent experiments. $^{****}P < 0.0001$; $^{***}P < 0.001$ one-way ANOVA followed by Tukey Mean Difference test.

The Δ*pil1* mutant was more affected than Δ*gup1*, which in turn was more affected than *wt*, while nearly all Δ*gup1* Δ*pil1* cells died upon treatment (Fig. 5A). Subsequently, the number of surviving cells presenting membrane disruption was determined by staining the cells with PI. The integrity of the plasma membrane and consequent impermeability to PI allows to discriminate between apoptotically or necrotically dying cells, although it does not discriminate between primary or secondary necrosis (Eisenberg *et al.* 2010; Carmona-Gutierrez *et al.* 2018). Results in Fig. 5B show the percentage of PI^+ cells. The *wt* and Δ*gup1* strains presented results similar to previously reported (Tulha *et al.* 2012). The decrease in viability of *wt* cells (~45%) was not accompanied by a correspondent increase in loss of plasma membrane integrity (~5%), which points to a RCD event. The decrease in cell survival observed in Δ*gup1*, on the other hand, was accompanied by loss of plasma membrane integrity as expected from cells mostly dying of a non-regulated death. The Δ*pil1* mutant presented a much smaller percentage of surviving c.f.u. (Fig. 5A), which displayed an intermediate percentage of cells that lost membrane integrity (Fig. 5B), suggesting that the fraction of the population dying necrotically could be dying of a secondary necrosis. Finally, the absence of both Gup1 and Pil1 almost killed the entire cell population, almost 100% of the cells being PI^+. The integrity of the membrane rafts and the distribution of ergosterol, which are so severely disrupted in Δ*pil1* (Walther *et al.* 2006; Grossmann *et al.* 2007, 2008) and in Δ*gup1* (Ferreira and Lucas 2008), were suggested to affect cell survival to acetic acid and induced apoptosis (Mollinedo 2012), although there is yet no mechanistic understanding. The results obtained here are consistent with the hypothesis that the disruption of eisosomes derived from *GUP1* and *PIL1* deletion could cause Fps1 to be improperly regulated (unable to

close properly), promoting death-inducing influx of acetic acid into cells.

FINAL REMARKS

The present work revealed the plasma membrane eisosome structural protein Pil1 as a new physical interaction partner of the MBOAT O-acyltransferase Gup1. *GUP1* deletion resulted in a substantial reduction of the number of eisosomes per cell, estimated by measuring the number of Pil1-GPF punctate patches, while the expression of *PIL1* and the Pil1 protein levels remained unchanged. Thus, Gup1 may be implicated in eisosome formation/assembly. Pil1 preferentially binds to a minor phospholipid present in the membranes—PI(4,5)P2. The Δ*gup1* mutant is affected in membrane composition, presenting less phospholipids, and more diacylglycerol (Oelkers *et al*. 2000), which can be obtained by PI(4,5)P2 hydrolysis. Thus, such alterations at the level of PI homeostasis could be the cause for the reduction in the number of eisosomes.

Phenotypical analyses of the single and double *GUP1* and *PIL1* mutants revealed that Gup1 and Pil1 interact genetically. This interaction was found to be mostly negative. Some of the phenotypes were aggravated or only visible in the double mutant. The cell wall injuring drugs CFW and CR impaired growth of the double mutant. Thus, Gup1 and Pil1 are functionally implicated in cell wall biogenesis, possibly through the CWI/PKC pathway, which is the common denominator of these drugs.

One well-documented consequence of the disruption in *PIL1* is the mislocalization of several important signaling effectors, namely, the Sho1 and Sln1 activators of the HOG pathway (Tanigawa *et al*. 2012). Accordingly, Δ*pil1* was shown here to be affected by salt stress. Hyperosmotic stress induces a HOG-mediated response culminating, among others, in the production and intracellular accumulation of the osmolyte glycerol (Hohmann 2009). Hyperosmotic stress also results in closure of Fps1 so that the cell can retain glycerol (Tamás *et al*. 1999). Hog1, the MAP kinase of the HOG-pathway, has been shown to act as a negative regulator of Fps1 activity (Thorsen *et al*. 2006; Lee *et al*. 2013). A lower activity of Hog1, due to mislocalization of Sho1 and Sln1, was expected to result in an increased number of open Fps1 molecules. Besides glycerol, Fps1 is also permeated by the trivalent metalloid ions arsenite and antimonite (Wysocki *et al*. 2001), xylitol (Tani, Tagushi and Akamatsu 2017) and acetic acid (Mollapour and Piper 2007). In this work, it is shown that the Δ*gup1* Δ*pil1* mutant accumulated elevated levels of arsenic and were As(III) sensitive. Furthermore, when exposed to toxic acetic acid concentration, Δ*pil1* dies much more than Δ*gup1*, and the double mutant is almost fully killed. Thus, acetic acid is most probably flooding the Δ*gup1* Δ*pil1* mutant, as observed to occur with arsenite. Whether the increased influx in the double mutant is indeed mediated by Fps1, as well as the molecular details of why Fps1 is deregulated in this strain, remains to be firmly established. We note that the proportion of acetic acid-induced cell death is not equivalent to the proportion of As(III) intake in either of the four yeast strains. The Δ*pil1* takes up approximately the same amount of arsenic as *wt*, but it dies almost 10× more of acetic acid, both strains dying of apoptosis. On the other hand, the deletion of *GUP1* causes a drastic change in this type of death, which becomes necrotic-like (Tulha *et al*. 2012). This is not maintained in the double mutant, in which the acetic acid-treated cells were almost all PI^+, implying that the deletion of *PIL1*, apparently epistatically reverts the necrosis-like death observed as the consequence of the deletion of *GUP1*. Thus, the mechanisms underlying the observed phenotypes are likely multifactorial.

Eisosomes delimit furrow-like membrane invaginations associated with MCC domains, which concentrate sphingolipids, sterols as well as signaling molecules involved in the regulation of (i) TORC2-Ypk1, by temporarily sequestering Slm1/2, therefore indirectly controlling sphingolipid synthesis (Berchtold *et al*. 2012); (ii) HOG pathway, interfering with the partitioning of the Sln1 and Sho1 sensors (Tanigawa *et al*. 2012); and (iii) CWI pathway, in which case eisosomes appear to be instrumental in sensing mechanical stress (Berchtold *et al*. 2012; Kabeche *et al*. 2014; Foderaro, Douglas and Konopka 2017). Previously, Gup1 protein was suggested to act at a hub between the CWI/PKC1, TORC2/YPK, TORC1/Pkh1/2 and HOG/Sho1 pathways in close association with PI(4,5)P2 (Lucas *et al*. 2016). This hypothesis is reinforced by the present results.

Summing up, this work presents evidence of physical, genetic and functional interactions between Gup1 and Pil1. Phenotypes associated with the deletion of *GUP1* are numerous and mostly common to those caused by *PIL1* deletion (compare Lucas *et al*. 2016 with Lanze *et al*. 2020). Phenotypes associated with the double deletion of these two proteins include defective acetic acid-promoted RCD, as well as arsenite uptake, suggesting that Fps1 might be deregulated in the absence of both proteins. Other phenotypes show that the interaction of these proteins affects cell wall integrity, the most prominent phenotype ever described in association with the deletion of *GUP1*. Most importantly, results show that the absence of Gup1 does not affect the expression of *PIL1* but strongly suggest it affects the number and size of eisosomes. *GUP1* deletion in the fungal pathogen *C. albicans* affects its virulence and ability to differentiate, adhere, invade and form biofilms (Ferreira *et al*. 2010). Thus, a better understanding of Gup1, its interaction partners and cellular functions might be useful for future development of antifungal drugs.

ACKNOWLEDGMENTS

We thank Gianluca Bleve, ISPA, Unità di Lecce, Italy, and Erin K. O'Shea, Howard Hughes Medical Institute, for kindly providing the pYES2-*GUP1-GFP* plasmid and the Δ*pil1-PIL1-GFP* strain, respectively.

SUPPLEMENTARY DATA

Supplementary data are available at *FEMSYR* online.

FUNDING

JT and MA-R are Ph.D. students from FCT (Fundação para a Ciência e Tecnologia), Portugal (grant numbers SFRH/BD/76025/2011 and SFRH/BD/145354/2019). This work was supported by the Marie Skłodowska-Curie Actions, Initial Training Network GLYCOPHARM (PITN-GA-2012-317297), and by the strategic programme UID/BIA/04050/2013 (POCI-01-0145-FEDER-007569) funded by national funds through the FCT and by the Eropean Regional Development Fund, through the COMPETE 2020. Work in the MJT laboratory was supported by the Swedish Research Council (grant numbers 621-2014-4597 and 348-2014-4296).

AUTHOR CONTRIBUTIONS

JT—acquisition and interpretation of the data; writing of the manuscript; MA-R, LAE and SR—acquisition of data; revising the manuscript; and CL and MJT—conception of the study; interpretation of the data; writing of the manuscript.

Conflict of Interest. None declared.

REFERENCES

Abe Y, Kita Y, Niikura T. Mammalian Gup1, a homolog of *Saccharomyces cerevisiae* glycerol uptake/transporter 1, acts as a negative regulator for N-terminal palmitoylation of Sonic Hedgehog. *FEBS Lett* 2008;**275**:318–31.

Ahmadpour D, Maciaszczyk-Dziubinska E, Babazadeh R *et al.* The mitogen-activated protein kinase Slt2 modulates arsenite transport through the aquaglyceroporin Fps1. *FEBS Lett* 2016;**590**:3649–59.

Alonso-Monge R, Navarro-García F, Molero G *et al.* Role of the mitogen-activated protein kinase Hog1p in morphogenesis and virulence of *Candida albicans*. *J Bacteriol* 1999;**181**:3058–68.

Berchtold D, Piccolis M, Chiaruttini N *et al.* Plasma membrane stress induces relocalization of Slm proteins and activation of TORC2 to promote sphingolipid synthesis. *Nat Cell Biol* 2012;**14**:542–7.

Bleve G, di Sansebastiano GP, Grieco F. Over-expression of functional *Saccharomyces cerevisiae GUP1*, induces proliferation of intracellular membranes containing ER and Golgi resident proteins. *Biochim Biophys Acta* 2011;**1808**:733–44.

Bleve G, Zacheo G, Cappello MS *et al.* Subcellular localization and functional expression of the glycerol uptake protein 1 (*GUP1*) of *Saccharomyces cerevisiae* tagged with green fluorescent protein. *Biochem J* 2005;**390**:145–55.

Bosson R, Jaquenoud M, Conzelmann A. *GUP1* of *Saccharomyces cerevisiae* encodes an *O*-acyltransferase involved in remodelling of the GPI anchor. *Mol Biol Cell* 2006;**17**:2636–45.

Carmona-Gutierrez D, Bauer MA, Zimmermann A *et al.* Guidelines and recommendations on yeast cell death nomenclature. *Microb Cell* 2018;**5**:4–31.

Douglas LM, Konopka JB. Fungal membrane organization: the eisosome concept. *Ann Rev Microbiol* 2014;**68**:377–93.

Douglas LM, Wang HX, Li L *et al.* Membrane compartment occupied by Can1 (MCC) and eisosome subdomains of the fungal plasma membrane. *Membranes* 2011;**1**:394–411.

Dupont S, Beney L, Ritt J-F *et al.* Lateral reorganization of plasma membrane is involved in the yeast resistance to severe dehydration. *Biochim Biophys Acta* 2010;**1798**:975–85.

Eisenberg T, Carmona-Gutierrez D, Buttner S *et al.* Necrosis in yeast. *Apoptosis* 2010;**15**:257–68.

Ferreira C, Lucas C. The yeast *O*-acyltransferase Gup1p interferes in lipid metabolism with direct consequences on the sphingolipid-sterol-ordered domains integrity/assembly. *Biochim Biophys Acta* 2008;**1778**:2648–53.

Ferreira C, Silva S, Faria-Oliveira F *et al.* *Candida albicans* virulence and drug-resistance requires the *O*-acyltransferase Gup1p. *BMC Microbiol* 2010;**10**:238.

Ferreira C, Silva S, van Voorst F *et al.* Absence of Gup1p in *Saccharomyces cerevisiae* results in defective cell wall composition, assembly, stability and morphology. *FEMS Yeast Res* 2006;**6**:1027–38.

Ferreira C, van Voorst F, Martins A *et al.* A member of the sugar transporter family, Stl1p is the glycerol/H^+ symporter in *Saccharomyces cerevisiae*. *Mol Biol Cell* 2005;**16**:2068–76.

Foderaro JE, Douglas LM, Konopka JB. MCC/eisosomes regulate cell wall synthesis and stress responses in fungi. *J Fungi* 2017;**3**:E61.

Fröhlich F, Christiano R, Olson DK *et al.* A role for eisosomes in maintenance of plasma membrane phosphoinositide levels. *Mol Biol Cell* 2014;**25**:2797–806.

García-Rodriguez LJ, Durán A, Roncero C. Calcofluor antifungal action depends on chitin and a functional high-osmolarity glycerol response (HOG) pathway: evidence for a physiological role of the *Saccharomyces cerevisiae* HOG pathway under noninducing conditions. *J Bacteriol* 2000;**182**:2428–37.

Gavin AC, Bösche M, Krause R *et al.* Functional organization of the yeast proteome by systematic analysis of protein complexes. *Nature* 2002;**415**:141–7.

Grossmann G, Malínský J, Stahlschmidt W *et al.* Plasma membrane microdomains regulate turnover of transport proteins in yeast. *J Cell Biol* 2008;**183**:1075–88.

Grossmann G, Opekarová M, Malínský J *et al.* Membrane potential governs lateral segregation of plasma membrane proteins and lipids in yeast. *EMBO J* 2007;**26**:1–8.

Habermann B. The BAR-domain family of proteins: a case of bending and binding? *EMBO Rep* 2004;**5**:250–5.

Hohmann S. Control of high osmolarity signalling in the yeast *Saccharomyces cerevisiae*. *FEBS Lett* 2009;**583**:4025–9.

Holst B, Lunde C, Lages F *et al.* *GUP1* and its close homologue *GUP2*, encoding multimembrane-spanning proteins involved in active glycerol uptake in *Saccharomyces cerevisiae*. *Mol Microbiol* 2000;**37**:108–24.

Huh W-K, Falvo JV, Gerke LC *et al.* Global analysis of protein localization in budding yeast. *Nature* 2003;**425**:686–91.

Ito H, Fukuda Y, Murata K *et al.* Transformation of intact yeast cells treated with alkali cations. *J Bacteriology* 1983;**153**:163–8.

Kabeche R, Howard L, Moseley JB. Eisosomes provide membrane reservoirs for rapid expansion of the yeast plasma membrane. *J Cell Science* 2015b;**128**:4057–62.

Kabeche R, Madrid M, Cansado J *et al.* Eisosomes regulate phosphatidylinositol 4,5-bisphosphate (PI(4,5)P2) cortical clusters and mitogen-activated protein (MAP) kinase signalling upon osmotic stress. *J Biol Chem* 2015a;**290**:25960–73.

Kabeche R, Roguev A, Krogan NJ *et al.* A Pil1-Sle1-Syj1-Tax4 functional pathway links eisosomes with PI(4,5)P2 regulation. *J Cell Sci* 2014;**127**:1318–26.

Karotki L, Huiskonen JT, Stefan CJ *et al.* Eisosome proteins assemble into a membrane scaffold. *J Cell Biol* 2011;**195**:889–902.

Kunkel J, Luo X, Capaldi AP. Integrated TORC1 and PKA signaling control the temporal activation of glucose-induced gene expression in yeast. *Nat Commun* 2019;**10**:3558.

Kuranda K, Leberre V, Sokol S *et al.* Investigating the caffeine effects in the yeast *Saccharomyces cerevisiae* brings new insights into the connection between TOR, PKC and Ras/cAMP signalling pathways. *Mol Microbiol* 2006;**61**:1147–66.

Lanze CE, Gandra RM, Foderaro JE *et al.* Plasma membrane MCC/eisosome domains promote stress resistance in fungi. *Microbiol Mol Biol Rev* 2020;**84**:e00063–19.

Lee J, Levin DE. Intracellular mechanism by which arsenite activates the yeast stress MAPK Hog1. *Mol Biol Cell* 2018;**29**:1904–15.

Lee J, Reiter W, Dohnal I *et al*. MAPK Hog1 closes the *S. cerevisiae* glycerol channel Fps1 by phosphorylating and displacing its positive regulators. *Genes Dev* 2013;**27**:2590–601.

Lee RT, Zhao Z, Ingham PW. Hedgehog signalling. *Development* 2016;**143**:367–72.

Lenardon M, Lesiak I, Munro CA *et al*. Dissection of the *Candida albicans* class I chitin synthase promoters. *Mol Gen Genom* 2009;**281**:459–71.

Levin DE. Cell wall integrity signalling in *Saccharomyces cerevisiae*. *Microbiol Mol Biol Rev* 2005;**69**:262–91.

Lewis JA, Broman AT, Will J *et al*. Genetic architecture of ethanol-responsive transcriptome variation in *Saccharomyces cerevisiae* strains. *Genetics* 2014;**198**:369–82.

Lindahl L, Genheden S, Faria-Oliveira F *et al*. Alcohols enhance the rate of acetic acid diffusion in *S. cerevisiae*: biophysical mechanisms and implications for acetic acid tolerance. *Microb Cell* 2017;**5**:42–55.

Lucas C, Ferreira C, Cazzanelli G *et al*. Yeast Gup1(2) proteins are homologues of the Hedgehog morphogens acyltransferases HHAT(L): facts and implications. *J Dev Biol* 2016;**4**:33.

Lum PY, Armour CD, Stepaniants SB *et al*. Discovering modes of action for therapeutic compounds using a genome-wide screen of yeast heterozygotes. *Cell* 2004;**116**:121–37.

Malínská K, Malínský J, Opekarová M *et al*. Distribution of Can1p into stable domains reflects lateral protein segregation within the plasma membrane of living *S. cerevisiae* cells. *J Cell Sci* 2004;**117**:6031–41.

Malínská K, Malínský J, Opekarová M *et al*. Visualization of protein compartmentation within the plasma membrane of living yeast cells. *Mol Biol Cell* 2003;**14**:4427–36

Malínský J, Opekarová M, Tanner W. The lateral compartmentation of the yeast plasma membrane. *Yeast* 2010;**27**:473–8.

Miller J, Lo RS, Ben-Hur A *et al*. Large-scale identification of yeast integral membrane protein interactions. *Proc Natl Acad Sci USA* 2005;**102**:12123–8.

Moharir A, Gay L, Appadurai D *et al*. Eisosomes are metabolically regulated storage compartments for APC-type nutrient transporters. *Mol Biol Cell* 2018;**29**:2113–27.

Mollapour M, Piper PW. Hog1 mitogen-activated protein kinase phosphorylation targets the yeast Fps1 aquaglyceroporin for endocytosis, thereby rendering cells resistant to acetic acid. *Mol Cell Biol* 2007;**27**:6446–56.

Mollinedo F. Lipid raft involvement in yeast cell growth and death. *Front Oncol* 2012;**2**:140.

Moreira KE, Walther TC, Aguilar PS *et al*. Pil1 controls eisosome biogenesis. *Mol Biol Cell* 2009;**20**:809–18.

Munro CA, Selvaggini S, de Bruijn I *et al*. The PKC, HOG and Ca^{2+} signalling pathways co-ordinately regulate chitin synthesis in *Candida albicans*. *Mol Microbiol* 2007;**63**:1399–413.

Oelkers P, Tinkelenberg A, Erdeniz N *et al*. A lecithin cholesterol acyltransferase-like gene mediates diacylglycerol esterification in yeast. *J Biol Chem* 2000;**275**:15609–12.

Oliveira R, Lucas C. Expression studies of *GUP1* and *GUP2*, genes involved in glycerol active transport in *Saccharomyces cerevisiae*, using semi-quantitative RT-PCR. *Curr Genet* 2004;**46**:140–6.

Olivera-Couto A, Graña M, Harispe L *et al*. The eisosome core is composed of BAR domain proteins. *Mol Biol Cell* 2011;**22**:2360–72.

Olivera-Couto A, Salzman V, Mailhos M *et al*. Eisosomes are dynamic plasma membrane domains showing Pil1-Lsp1 heteroligomer binding equilibrium. *Biophys J* 2015;**108**:1633–44.

Ram AFJ, Klis FM. Identification of fungal cell wall mutants using susceptibility assays based on Calcofluor White and Congo Red. *Nat Prot* 2006;**1**:2253–6.

Rodríguez-Peña JM, García R, Nombela C *et al*. The high-osmolarity glycerol (HOG) and cell wall integrity (CWI) signalling pathways interplay: a yeast dialogue between MAPK routes. *Yeast* 2010;**27**:495–502.

Roncer C, Durán A. Effect of Calcofluor White and Congo Red on fungal cell wall morphogenesis:*in vivo* activation of chitin polymerization. *J Bacteriol* 1985;**163**:1180–5.

Schmittgen TD, Livak KJ. Analyzing real-time PCR data by the comparative C(T) method. *Nat Prot* 2008;**3**:1101–8.

Strádalová V, Stahlschmidt W, Grossmann G *et al*. Furrow-like invaginations of the yeast plasma membrane correspond to membrane compartment of Can1. *J Cell Sci* 2009;**122**:2887–94.

Tamás MJ, Luyten K, Sutherland FC *et al*. Fps1p controls the accumulation and release of the compatible solute glycerol in yeast osmoregulation. *Mol Microbiol* 1999;**31**:1087–104.

Tanigawa M, Kihara A, Terashima M *et al*. Sphingolipids regulate the yeast high-osmolarity glycerol response pathway. *Mol Cell Bio* 2012;**14**:2861–70.

Tani T, Tagushi H, Akamatsu T. Analysis of metabolisms and transports of xylitol using xylose- and xylitol-assimilating *Saccharomyces cerevisiae*. *J Biosci Bioeng* 2017;**123**:613–20.

Thorsen M, Di Y, Tängemo C *et al*. The MAPK Hog1p modulates Fps1p-dependent arsenite uptake and tolerance in yeast. *Mol Biol Cell* 2006;**17**:4400–10.

Tulha J, Faria-Oliveira F, Lucas C *et al*. Programmed cell death in *Saccharomyces cerevisiae* is hampered by the deletion of *GUP1* gene. *BMC Microbiol* 2012;**12**:80.

Tulha J, Lucas C. *Saccharomyces cerevisiae* mitochondrial voltage 1 dependent anion channel (VDAC) Por1 interacts physically with the MBOAT O-acyltransferase Gup1/HHATL in the control of cell wall integrity and programmed cell death. *FEMS Yeast Res* 2018;**18**:foy097.

van Zeebroeck G, Kimpe M, Vandormael P *et al*. A split-ubiquitin two-hybrid screen for proteins physically interacting with the yeast amino acid transceptor Gap1 and ammonium transceptor Mep2. *PLoS One* 2011;**6**:e24275.

Varjosalo M, Taipale J. Hedgehog signaling. *J Cell Sci* 2007;**120**:3–6.

Walther TC, Brickner JH, Aguilar PS *et al*. Eisosomes mark static sites of endocytosis. *Nature* 2006;**439**:998–1003.

Wang HX, Douglas LM, Aimanianda V *et al*. The *Candida albicans* Sur7 protein is needed for proper synthesis of the fibrillar component of the cell wall that confers strength. *Eukaryot Cell* 2011;**10**:72–80.

Wanke V, Cameroni E, Uotila A *et al*. Caffeine extends yeast lifespan by targeting TORC1. *Mol Microbiol* 2008;**69**:277–85.

Wysocki R, Chéry CC, Wawrzycka D *et al*. The glycerol channel Fps1p mediates the uptake of arsenite and antimonite in *Saccharomyces cerevisiae*. *Mol Microbiol* 2001;**40**:1391–401.

Ziółkowska NE, Karotki L, Rehman M *et al*. Eisosome-driven plasma membrane organization is mediated by BAR domains. *Nat Str Mol Biol* 2011;**18**:854–6.